

Are your MRI contrast agents cost-effective?

Learn more about generic Gadolinium-Based Contrast Agents.



FRESENIUS  
KABI

caring for life

**AJNR**

## The MR Imaging Appearance of the Vascular Pedicle Nasoseptal Flap

M.D. Kang, E. Escott, A.J. Thomas, R.L. Carrau, C.H. Snyderman, A.B. Kassam and W. Rothfus

*AJNR Am J Neuroradiol* 2009, 30 (4) 781-786

doi: <https://doi.org/10.3174/ajnr.A1453>

<http://www.ajnr.org/content/30/4/781>

This information is current as of April 19, 2024.

M.D. Kang  
E. Escott  
A.J. Thomas  
R.L. Carrau  
C.H. Snyderman  
A.B. Kassam  
W. Rothfus

## The MR Imaging Appearance of the Vascular Pedicle Nasoseptal Flap

**BACKGROUND AND PURPOSE:** Recently, surgeons have used an expanded endonasal surgical approach (EENS) to access skull base lesions not previously accessible by minimally invasive techniques. Reconstruction of the large skull base defects created during EENS is necessary to prevent postoperative CSF leaks. A vascular pedicle nasoseptal mucoperiosteal flap based on the nasoseptal artery, (Hadad-Bassagasteguy flap) is becoming a common reconstructive technique. The purpose of this study was to review the expected MR imaging appearance of these flaps and to discuss variations in the appearance that may suggest potential flap failure.

**MATERIALS AND METHODS:** We retrospectively reviewed 10 patients who underwent EENS for resection of sellar lesions with skull base reconstruction by multilayered reconstruction including the Hadad-Bassagasteguy flap. All patients had preoperative, immediate, and delayed postoperative MR imaging scans. Flap features that were evaluated included flap configuration, signal intensity characteristics on T1-weighted and T2-weighted images, enhancement patterns, location, and flap thickness.

**RESULTS:** All patients had detectable postoperative skull base defects. All patients had C-shaped configuration flaps within the operative defect, which were isointense on T1-weighted and T2-weighted images on both immediate and delayed postoperative MR imaging scans. On the immediate scans, 8 of 10 patients had enhancing flaps and 2 of 10 had minimal to no enhancement. There were 9 of 10 patients who had enhancing flaps on delayed scans, and 2 of 10 patients had flaps that increased in enhancing coverage on the delayed scans.

**CONCLUSIONS:** Vascular pedicle nasoseptal flaps have a characteristic MR imaging appearance. It is important for the radiologist to recognize this appearance and to evaluate for variations that may suggest potential flap failure.

The standard trans-sphenoidal endoscopic approach is being increasingly used for the resection of sellar lesions. Recently, the surgical armamentarium has been augmented by expanded endonasal surgical approaches (EENS) that can provide access not only to lesions along the sagittal plane of the skull base (from the crista galli to the odontoid process), but also to parasellar and intracranial pathology. This has been made possible by the development of accurate and reliable surgical navigation systems; enhancement of the rod lens endoscope optics; improved resolution of digital cameras; and, perhaps most importantly, a multidisciplinary approach.<sup>1-3</sup>

Expanded endonasal surgical approaches can be divided into 4 sagittal plane corridors: transcribiform, tranplanum, trans-sellar, and transclival. These corridors allow endoscopic access to the entire ventral skull base.<sup>1-3</sup> There is a common initial nasal corridor, which entails removal of 1 middle turbinate, wide bilateral sphenoidotomies, and a posterior septectomy. This exposure allows visualization of critical surgical landmarks: the planum sphenoidale, clival indentation, internal carotid arteries, optic nerve canals, and the medial and

lateral optic-carotid recesses. Any of the 4 corridors can then be accessed expanding this initial exposure as seen in Fig 1.

Effective reconstruction of the tissue barriers between the arachnoid space and the sinonasal cavity has been a major challenge that initially hindered the use of the endonasal surgical approach beyond the sella turcica. For expanded endonasal approaches to become a viable surgical option, this issue needed to be addressed.<sup>4-7</sup> Reconstruction of small defects of the anterior skull base can be reliably performed with a variety of known techniques with a high degree of success (> 95%).<sup>5</sup> However, these techniques of dural closure were insufficient to repair the larger defects produced during EENS, thus leading to a high rate of postoperative CSF leaks.<sup>5,6</sup> Subsequently, vascular flaps were used to promote more rapid and complete healing after expanded endonasal surgery. Vascularized flaps include extranasal flaps such as the transpterygoid temporoparietal flaps; however, this flap requires a separate external approach, which adds to the complexity and morbidity of the procedure.<sup>6</sup>

Subsequently, the use of a multilayered reconstruction that includes a vascular pedicle flap of nasal septum mucoperiosteum or mucoperichondrium based on the nasoseptal artery, a branch of the posterior septal artery, and the terminal branch of the internal maxillary artery<sup>5-7</sup> was adopted. Its use has led to a sharp decrease in the incidence of postoperative CSF leaks after expanded endoscopic surgery.<sup>6,7</sup>

During the reconstructive phase, a multilayer reconstruction is used with an inlay subdural graft and, occasionally, an onlay graft of fat or fascia. The nasoseptal flap can be applied directly to the dura as seen in Fig 2 or occasionally may be placed over fat. Then a biologic glue helps to fix the flap, and a nasal sponge packing or a 14F Foley balloon catheter is in-

Received August 10, 2008; accepted after revision November 10.

From the Department of Neuroradiology (M.D.K.), Thomas Jefferson University Hospital, Philadelphia, Pa; and Departments of Neuroradiology (E.E., W.R.), Neurosurgery (A.J.T., R.L.C., C.H.S., A.B.K.), and Otolaryngology—Head & Neck Surgery (R.L.C., C.H.S., A.B.K.), University of Pittsburgh Medical Center, Pittsburgh, Pa.

Previously presented at: Annual Meeting of the American Society of Head and Neck Radiology, September 26, 2007, Seattle, Wash.

Please address correspondence to Melissa Kang, MD, Department of Neuroradiology, Thomas Jefferson University Hospital, 111 South 11th St, Philadelphia, PA 19107; e-mail: Melissa.kang@jefferson.edu

DOI 10.3174/ajnr.A1453

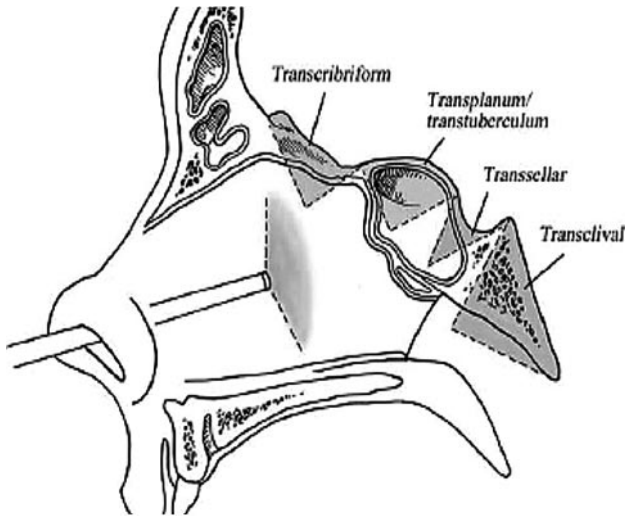


**Fig 1.** Drawing of the 4 corridors via an expanded endoscopic approach to the skull base in the sagittal plane. Reprinted with permission from the *Journal of Neurosurgery Pediatric* (2007;106:75–86).



**Fig 2.** Coronal drawing of a vascular pedicled nasoseptal flap covering defect in the planum sphenoidale. The configuration is C shaped. There is an antrostomy defect (\*) and the nasal septum (NS). Reprinted with permission from *Neurosurgery* (2008;63:ONS44-ONS53).

serted under endoscopic guidance to hold the flap in place. The entire reconstruction may be supported in place by an inflated Foley catheter balloon (Fig 3).

The purpose of this study was to describe the expected MR imaging appearance of the vascular pedicled nasoseptal flap and to evaluate for variations that may predict potential flap failure.

### Materials and Methods

After approval by our institutional review board, we retrospectively reviewed the imaging and clinical data of 10 patients who underwent an endoscopic resection of sellar lesions and a skull base reconstruction with use of a vascular pedicle nasoseptal flap during 12 months (January 2006 to January 2007). Inclusion criteria consisted of patients who had sella-based masses, with or without involvement of the suprasellar cistern and with or without cavernous sinus extension. In essence, patients were limited to trans-sellar or transtubercular endonasal surgery. Imaging criteria were defined by consensus of 3 neuro-radiologists, 2 of whom are CAQ certified, and individual cases were then evaluated by a single neuroradiologist.

All patients had a preoperative MR imaging examination, an im-

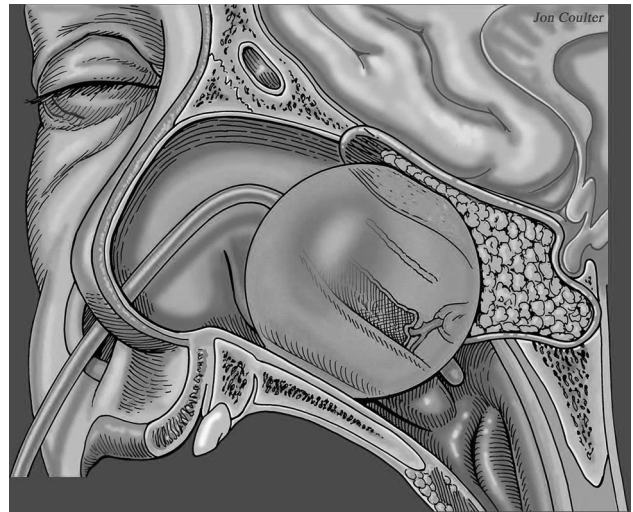


**Fig 3.** Sagittal drawing of the vascular pedicled nasoseptal flap covering the surgical defect with packing material and a Foley catheter balloon securing the flap in place. Reprinted with permission from *Neurosurgery* (2008;63:ONS44-ONS53).

mediate postoperative scan during the first 48 hours postoperatively, and a delayed postoperative MR imaging examination at a 3- to 7-month interval (average, 4.5 months). MR imaging included the following sequences outlined in Table 1: sagittal T1-weighted, coronal T1-weighted, and axial T2 fast spin-echo, and sagittal T1-weighted and coronal T1-weighted postcontrast with fat saturation focused on the sella turcica. Axial 3D spoiled gradient-recalled acquisition post-contrast images were obtained of the entire brain. Enhanced images were obtained with the use of intravenous Multihance contrast (Bracco Diagnostic, Princeton, NJ). The average dose for the immediate postoperative scan was 14.9 mL (range, 7–17 mL). In 2 patients, the dose was not documented.

The average dose for follow-up MR imaging scans at 3 to 7 months was 9 mL (range, 7–13 mL). The difference in the average doses was the result of 2 patients who had received a double dose on their immediate postoperative scan. All examinations were performed on a 1.5T MR unit (GE Healthcare, Milwaukee, Wis). Features of the flap appearance, which were evaluated, include flap configuration, signal intensity characteristics on T1-weighted and T2-weighted images, enhancement patterns, location, and flap thickness; this correlated with postoperative clinical course and complications.

### Results

All 10 patients had detectable skull base defects. Flaps isointense on T1-weighted and T2-weighted sequences on both immediate and follow-up postoperative MR imaging scans (Table 2) were evident in all patients. A C-shaped configuration of the flap subjacent to the operative skull base defect on both the coronal and sagittal projections was demonstrated in all patients. Enhancing flaps on immediate postoperative scans were evident in 8 of 10 patients, and no enhancement on immediate postoperative scans but enhancement on delayed MR imaging scan was noted in 2 of 10 patients. There were flaps that enhanced on delayed follow-up MR imaging scans in 9 of 10 patients. In the 1 patient in whom there was no enhancement on the delayed follow-up MR imaging scan, enhancement was evident on the immediate postoperative MR imaging scan. Two patients had flaps that increased in

**Table 1: MR imaging protocol on 1.5T magnet**

	Pulse Sequence	TE (ms)	TR (ms)	FOV (cm)	Thickness (mm)	Gap/Overlap (mm)	Fat Suppression (Y/N)	Contrast (Y/N)
Precontrast								
Sag T1	FSE	Min	<600	20	3	0.5	No	N
Cor T1	FSE	Min	<600	16	3	0.5	N	N
Ax T2	FSE	102	3400	22	5	1	Y	N
Postcontrast								
Cor T1	FSE	Min	<600	16	3	0.5	Y	Y
Sag T1	FSE-XL	Min	<600	20	3	0.5	Y	Y
Ax	3D SPGR	Min	Min	25	1.5	–	N	Y

**Note:**—Sag indicates sagittal; Cor, coronal; Ax, axial; FSE, fast spin-echo; N, no; Y, yes; SPGR, spoiled gradient-recalled echo.

**Table 2: Enhancement patterns of the vascular pedicle nasoseptal flap on immediate and delayed postoperative MR images**

Patient No. and Condition	Flap Enhancement		Average Flap Thickness Immediate Postoperative MR Image (mm)	Average Flap Thickness Follow-up Postoperative MR Image (mm)
	Immediate Postoperative MR Image (Y/N)	Follow-up Postoperative MR Image (Y/N)		
1. Pituitary microadenoma	Y	Y	5	7
2. Pituitary apoplexy	Y	Y	5	3.5
3. Pituitary macroadenoma	Y	Y	6	3
4. Pituitary microadenoma	Y	Y	4	3
5. Pituitary macroadenoma with hemorrhage	Y	Y	3	4
6. Pituitary microadenoma	Y	N	2.5	–
7. Pituitary microadenoma	N	Y	–	2
8. Pituitary macroadenoma	N	Y	–	3
9. Pituitary microadenoma	Y	Y	6	4
10. Pituitary macroadenoma	Y	Y	4	3

**Note:**—N indicates no; Y, yes.

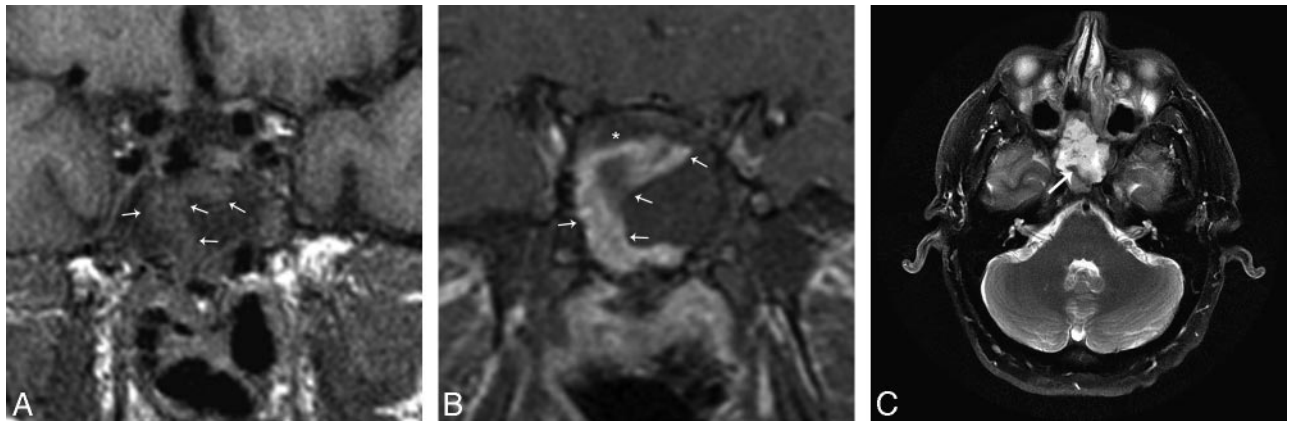


**Fig 4.** A, Immediate postoperative MR imaging. Coronal T1-weighted 3-mm precontrast image shows the nasoseptal flap (white arrows) subjacent to the surgical defect and is isointense. B, Immediate postoperative MR imaging. Coronal T1-weighted 3-mm postcontrast image with fat suppression shows a C-shaped enhancing nasoseptal flap (white arrows) underlying the surgical defect. There is linear hypointense, nonenhancing material deep to the flap, which represents the inlay and onlay graft material (\*). C, Immediate postoperative MR imaging axial T2-weighted 5 mm sequence with fat suppression shows an isointense curvilinear flap (white arrow) in the surgical defect. There is slightly hyperintense material deep to the flap, which is multilayer reconstruction material (\*). The T2 hyperintense material superficial to the flap is postoperative debris and fluid. This is a fat-suppressed image; as such, the hyperintense material is not fat packing.

enhancement anteriorly on the follow-up MR imaging scan (Table 2).

Eight of 10 patients received similar contrast dose for the immediate and delayed follow-up postoperative scans. Two remaining patients received a double dose for the immediate postoperative scan and a single dose for the follow-up scan. In 2 patients, the contrast doses were not documented on the immediate postoperative scan. However, significant changes in enhancement, either in thickness or in coverage area, were not exhibited in these patients. A postoperative CSF leak did not develop in any of the patients.

In addition to the vascular pedicle flap, there may be a

multilayer free tissue graft reconstruction consisting of an inlay subdural graft of collagen matrix and, occasionally, an onlay graft of fascia, or abdominal free fat. The appearance of the multilayer reconstruction is hypointense on T1-weighted sequences (Fig 4B) and slightly hyperintense on T2-weighted sequences deep to the flap (Fig 4C). Fat may or may not be present deep to the flap or may be placed superficial to the vascular pedicle flap as temporary packing. Then, the entire reconstruction may be secured in place with an inflated Foley balloon catheter, which is removed 3 to 5 days after surgery.

In the immediate postoperative MR imaging scans, the thickness of the flaps varied from nonvisualization, because of

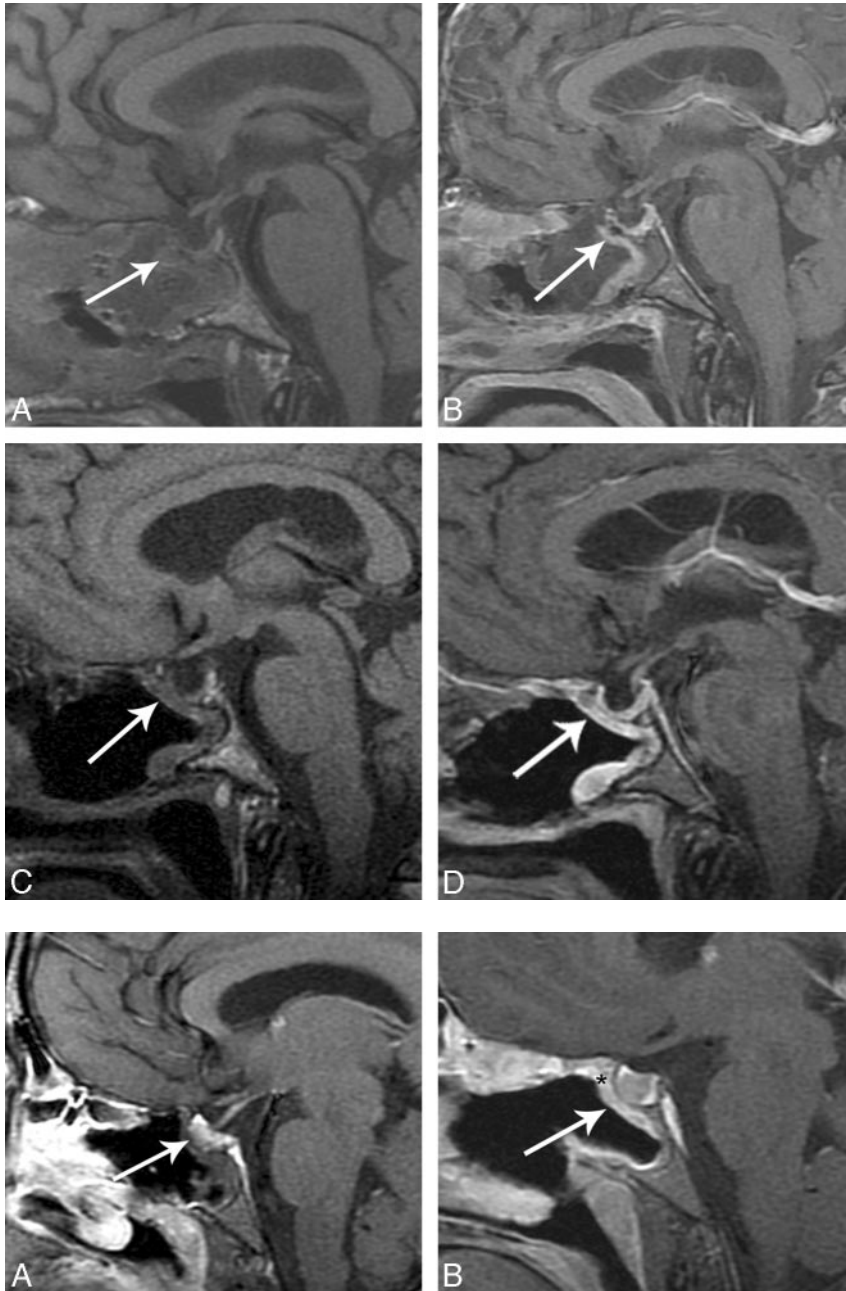


**Fig 5.** A, Immediate postoperative sagittal T1-weighted image shows a C-shaped flap underlying the operative defect (white arrow). B, Immediate postoperative sagittal T1-weighted image postcontrast with fat suppression shows a C-shaped flap underlying the operative defect (white arrow). C, Follow-up postoperative MR imaging scan sagittal unenhanced T1-weighted MR imaging shows decreased debris and removal of Foley catheter balloon in the sinonasal cavity and a C-shaped configuration of the flap, which is isointense (white arrow). D, Follow-up MR imaging sagittal T1-weighted postcontrast with fat suppression shows robust and thicker enhancement of the flap (white arrow).

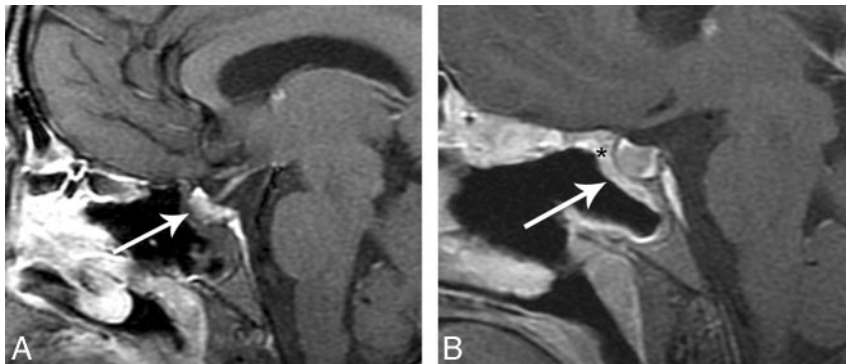


**Fig 6.** This example is from another data group but illustrates how a flap may be displaced. A, Immediate postoperative sagittal T1-weighted MR imaging precontrast shows no enhancing nasoseptal flap in the expected region (white arrow). B, Immediate postoperative sagittal T1-weighted MR imaging postcontrast with fat suppression shows no enhancing C-shaped flap underlying the surgical defect (white arrowhead). There is linear soft tissue along the undersurface of the Foley balloon (small white arrow). This is presumed to represent a displaced enhancing flap. A CSF leak developed in this patient.

lack of enhancement, to 5 mm, with an average of 4.4 mm (8 enhancing flaps).

The enhancement and average thickness of the flap in the immediate postoperative period can be variable (Table 2). There was mild enhancement of the flap in the immediate postoperative period in 1 of 10 patients, but on follow-up MR images, there was increased enhancement and thickness. Figure 5A shows a thin, enhancing C-shaped structure in the operative defect, which is thicker and more robust on follow-up MR imaging (Fig 5B). There was no appreciable enhancement on the immediate postoperative image (Fig 6A) in 1 of 10 patients. The follow-up MR imaging examination shows enhancement in the expected region of the flap (Fig 6B). A postoperative CSF leak did not develop in either of these patients.

The expected delayed postoperative follow-up MR imaging examination obtained at 3 to 7 months postoperatively (aver-

age, 4.5 months) showed resolution of the sinonasal cavity fluid and removal of the Foley catheter balloon. The signal intensity of the flap remained isointense on T1-weighted and T2-weighted sequences. The vascular pedicle nasoseptal flap was directly subjacent to the operative defect and may have been thicker or thinner with enhancement. The thickness of the multilayer reconstruction between the graft and the defect is decreased, demonstrating decreased postoperative edema and involution of the packing material (Fig 5D).

The average flap thickness on the delayed follow up MR imaging examination varied from nonvisualization to 7 mm. Three of 10 flaps were thicker and enhancing, whereas 6 of 10 flaps were thinner and enhancing. There was an increase in enhancement anteriorly in 2 of 10 patients (Table 2). One flap had minimal to no enhancement but did have enhancement on the immediate postoperative scan. This patient did not have a CSF leak.

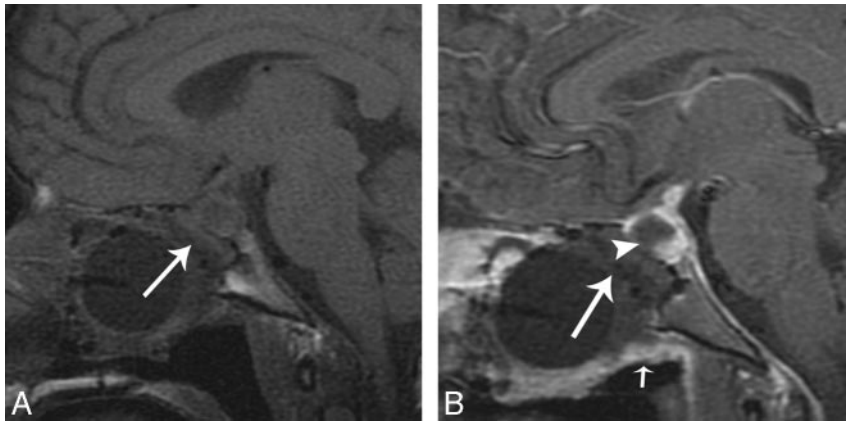


**Fig 7.** This example is from another data group but illustrates how flaps can be displaced and not adhere to the denuded sinonasal wall. *A*, Immediate postoperative coronal MR imaging T1-weighted postcontrast with fat suppression shows a defect (*white arrowhead*) left of the enhancing flap (*white arrow*). The flap (*white arrow*) is sloping inferiorly and is not in contact with the denuded sinonasal wall. A Foley catheter balloon is attempting to secure the flap. There is a large anterior skull base defect with herniation of brain parenchyma (*white curved arrow*). There is fat suppression making the defect (*white arrowhead*) look larger, which is a potential pitfall. The flap is displaced inferiorly on the left. This patient had a leak. *B*, Axial T1-weighted 5-mm MR imaging of no fat suppression shows the fat packing in the left defect (*black star*). This image demonstrates a potential pitfall when there is fat packing in overdiagnosing a defect on the fat-suppressed images.

## Discussion

Dural defects from EENS can vary in size and shape. The vascular pedicled nasoseptal flap can be harvested in varying sizes and shapes to match the anticipated operative defect resulting from a single expanded endonasal approach.<sup>6,7</sup> The flap must be harvested during the initial nasal corridor of surgery because it typically requires a posterior septectomy, which would destroy the vascular pedicle of the flap. The flap may be harvested from either or both sides of the nasal septum.

Two parallel incisions are performed. The inferior incision follows the maxillary crest, and the superior incision is 1 to 2 cm below the olfactory sulcus. Preservation of 1 to 2 cm of the superior septal mucosa preserves olfactory function. A joining vertical incision is made anterior to the anterior head of the inferior turbinate. The inferior incision extends following the posterior septum free edge, then crossing the posterior choana below the floor of the sphenoid sinus. The superior incision crosses the rostrum of the sphenoid at the level of the natural ostium of the sphenoid sinus. The flap is designed according to the size and shape of the anticipated defect.

During the extirpative phase, the nasoseptal flap is stored in the posterior nasopharynx or the maxillary antrum for clival, paraclival, or nasopharyngeal lesions. For storage in the maxillary antrum, a wide nasoastral window is created (Fig 2).

During the reconstructive phase, the vascular pedicled flap is applied directly over the dural defect or over an inlay graft and is held in place by an inflated Foley balloon catheter.

Variation in enhancement patterns were noted on the immediate and delayed postoperative MR imaging examinations. There were thinner enhancing flaps in 6 of the 10 patients, whereas there was thicker enhancement in 3 of the 10 patients. It was noted on follow-up endoscopic evaluation that, in general, the flaps tended to contract in size, which correlates with a finding of a thinner, enhancing flap. Furthermore, granulation tissue was also noted in the operative bed, which may explain the apparent increase in thickness of the enhancement on the delayed scans. An alternative possibility is increased mucosalization of the flap.

Nonenhancement may be the result of vascular compromise. The vascular supply may be compromised because of injury or compression. Therefore, inflation of the Foley catheter balloon is performed under endoscopic observation, as overinflation can compromise the vascular pedicle<sup>6</sup> as well as possibly compress intracranial structures. There can be variations in

the flap enhancement, particularly on both the immediate and delayed postoperative scans.

The variations of enhancement are difficult to correlate with flap failure because there is overlap in the imaging appearance of an enhancing flap and granulation tissue, particularly on the delayed scans. The immediate postoperative images would be more helpful to evaluate the enhancement of the flap because there would be less time for granulation tissue to form. In this group of patients with a small operative defect, the determination of flap failure was a CSF leak. This is an insensitive, however specific, end point for evaluation of flap survival in this group of patients. In 1 patient, there was no flap enhancement on the immediate postoperative examination, but there was enhancement on the delayed examination (Fig 6A). It is unclear if the enhancement is related to viable flap or to granulation tissue. A small operative defect may not necessitate a vascular flap for adequate closure; thus, a leak may not develop in a potentially nonviable flap. The enhancement pattern may be a more powerful predictor of flap failure in larger skull base defects.

Flap migration or displacement from the operative defect can be another potential cause of flap failure. If the mucoperichondrial surface is not opposed to the denuded sinonasal cavity, it will desiccate and contract. Areas at risk for migration are along the superior margin of the operative defect.<sup>6</sup> Flap displacement was thought to be the cause of flap failure in the patient in whom a CSF leak developed (Fig 7A-B) from an alternate dataset. Figure 7A shows no expected enhancing flap in the operative defect. Instead, there is an enhancing linear structure that is subjacent to the Foley balloon catheter. This structure likely represents a displaced flap.

On occasion, free fat is placed between the skull base defect and the sinonasal cavity. As long as the nasoseptal flap is in contact with denuded skull base along the margins of the defect, it will heal.<sup>6</sup> If fat is placed deep to the flap, it is placed such that it is not interposed between the margins of the denuded sinonasal cavity and the flap. Fat may also be placed superficial to the flap as temporary packing.

The presence of fat can be confirmed with the use of the fat suppression technique. Immediate postoperative images show fluid or blood in the sinonasal cavity and an inflated Foley catheter balloon (removed at postoperative days 3–5) securing the fat and the flap onto the operative defect. The material deep to and superficial to the flap can be seen separate from the

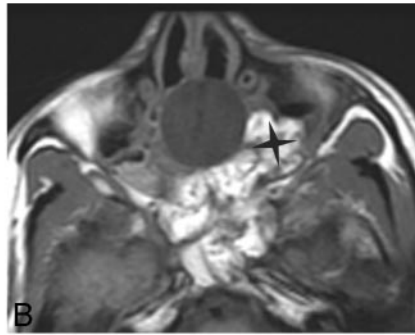
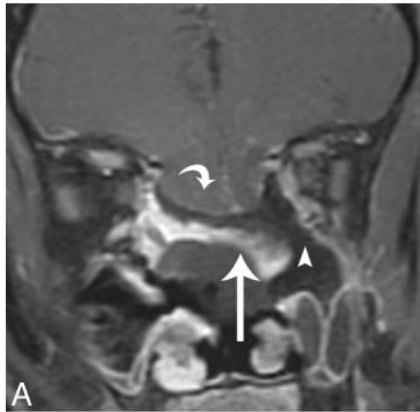


**Fig 8.** This example is from another data group but illustrates how flaps can migrate and not adhere to the denuded sinonasal wall. *A*, Immediate postoperative coronal MR imaging T1-weighted postcontrast with fat suppression shows a defect (white arrowhead) left of the enhancing flap (white arrow). The flap (white arrow) is sloping inferiorly and is not in contact with the denuded sinonasal wall. A Foley catheter balloon is attempting to secure the flap. There is a large anterior skull base defect with herniation of brain parenchyma (white curved arrow). Fat suppression is making the defect (white arrowhead) look larger, which is a potential pitfall. The flap is displaced inferiorly on the left. This patient had a leak. *B*, Axial T1-weighted MR imaging of no fat suppression shows the fat packing in the left defect (black star). This image demonstrates a potential pitfall when there is fat packing in overdiagnosing a defect on the fat-suppressed images.

flap, having different imaging characteristics and generally no enhancement.

An example of this type of flap failure is seen in Fig 8A-B in a patient in whom a CSF leak developed. This case demonstrates a large anterior skull base defect with fat packing between the enhancing flap and the denuded sinonasal wall. The flap is oriented inferiorly. Foreign bodies between the flap and the denuded sinonasal cavity, such as bone wax and surgical clips, can cause failure. MR imaging may not always detect these materials and occasionally may not be sensitive to this cause of failure.

Another cause of flap failure is a rotated flap. Flaps that are rotated with the mucosal surface facing the defect rather than facing the sinonasal cavity will not heal. In these cases, the MR imaging findings will show a normal enhancing flap. MR imaging cannot differentiate the mucosal surface from the mucoperichondrial surface and, therefore, will be insensitive to this cause of failure.<sup>6</sup>

#### Limitations and Future Considerations

We focused our patient selection criteria on trans-sellar/trans-tubercular approaches to pituitary macroadenomas to evaluate the MR imaging appearance of the vascular pedicle nasoseptal flap with as few confounding variables as possible. We understand that the dural defects created in these procedures may not necessitate the vascular flap for adequate closure.<sup>8,9</sup> Adequate closure is defined as no CSF leak. Therefore, it is unclear whether the flaps that did not enhance would have failed in patients with larger skull base defects and succeeded in the cases of patients with smaller defects, which did not necessitate a vascular flap for adequate closure. However, the understanding of the vascular flap and its appearance with as few variables allows for a starting point in the understanding of its expected MR imaging appearance.

Limitations of our study included small sample size, which did not include patients who had undergone more extensive expanded endonasal surgery, and a variable interval to the second postoperative MR imaging. It should be noted that the major benefit of the vascular pedicle nasoseptal flap is to reconstruct large skull base defects incurred during EENS and to promote faster and more complete healing.<sup>6,7</sup>

Future considerations include evaluation of the postradiation flap. Many of these patients are oncologic patients who

receive postoperative radiation and surveillance imaging for recurrence. Therefore, knowledge of the MR imaging appearance of the irradiated flap would allow the radiologist to avoid mistaking it for a recurrent or persistent pathologic condition. Moreover, the vascular pedicle nasoseptal flap may facilitate the mucosalization of the adjacent denuded areas. Conversely, mucocoeles or retention cysts may develop in viable mucosa trapped between the defect and the flap.

Additional follow-up studies can be performed to understand the evolution of the MR imaging appearance of a vascular pedicle nasoseptal flap and help predict potential flap failures.

#### Conclusions

Vascular pedicle nasoseptal flaps have a characteristic MR imaging appearance. It is important for the radiologist to recognize this appearance and evaluate for variations that may potentially predict flap failure.

#### References

- Kassam A, Thomas AJ, Snyderman C, et al. Fully endoscopic expanded endonasal approach treating skull base lesions in pediatric patients. *J Neurosurg* 2007;106 (2 Suppl):75–86
- Kassam AB, Gardner P, Snyderman C, et al. Expanded endonasal approach: fully endoscopic, completely transnasal approach to the middle third of the clivus, petrous bone, middle cranial fossa, and infratemporal fossa. *Neurosurg Focus* 2005;19:E6
- Kassam A, Snyderman CH, Mintz A, et al. Expanded endonasal approach: the rostrocaudal axis. Part I. Crista galli to the sella turcica. *Neurosurg Focus* 2005;19:E3.
- Kassam A, Carrau RL, Snyderman CH, et al. Evolution of reconstructive techniques following endoscopic expanded endonasal approaches. *Neurosurg Focus* 2005;19:E8
- Hadad G, Bassagasteguy L, Carrau RL et al. A novel reconstructive technique after endoscopic expanded endonasal approaches: vascular pedicle nasoseptal flap. *Laryngoscope* 2006;116:1882–86
- Kassam A, Thomas A, Carrau R, et al. Endoscopic reconstruction of the skull base using a pedicled nasoseptal flap. *Neurosurgery* 2008;63(1 Suppl 1): ONS44–52; discussion ONS52–53
- Pinheiro-Neto CD, Prevedello DM, Carrau RL, et al. Improving the design of the pedicled nasoseptal flap for skull base reconstruction: a radioanatomic study. *Laryngoscope* 2007;117:1560–69
- Shiley SG, Limonadi F, Delashaw JB, et al. Incidence, etiology, and management of cerebrospinal fluid leaks following trans-sphenoidal surgery. *Laryngoscope* 2003;113:1283–88
- Cappabianca P, Cavallo LM, Esposito F, et al. Sellar repair in endoscopic endonasal transsphenoidal surgery: results of 170 cases. *Neurosurgery* 2002;51: 1365–71; discussion 1371–72